New Zealand Journal of Marine and Freshwater Research, 1992, Vol. 26: 37–51
0028–8330/2601–0037

Modelling ocean temperatures and mixed-layer depths in the Tasman Sea off the South Island, New Zealand

STEFAN RAHMSTORF
New Zealand Oceanographic Institute
DSIR Marine and Freshwater
Department of Scientific and Industrial Research
Private Bag, Kilbirnie
Wellington, New Zealand

*Present address: Institut für Meereskunde, Düsternbrooker Weg 20, 23 Kiel, Germany.

Abstract A vertical mixing model was applied to a location off the west coast of the South Island, New Zealand, with the aim of simulating the seasonal cycle of temperature and mixed layer depth in the region. Observed weather data for 1973–89 were used to drive the model. Model results for sea temperature and mixed layer depth were compared to measurements from ships, moored temperature sensors, and satellites. The main features of the variations in temperature and mixed layer depth can be explained by the local meteorological forcing and vertical mixing, together with a general southward flow in the study area. Superimposed are short-term variations which are obviously related to variable currents and the associated horizontal heat transport.

Keywords sea temperature; mixed layer; computer model; seasonal cycles; remote sensing; advection

INTRODUCTION

A focus of oceanographic research in New Zealand in the 1980s was the area off the west coast of the South Island. This area is a major fishing ground and spawning area for hoki (*Macruronus novaezelandiae*), an important commercial fish species. Several research cruises to the area have focused on primary production, phytoplankton, and hoki larvae and their dependence on physical parameters. The two Tasman Boundary Experiment (TASBEX) cruises in November 1986 and May 1987 were devoted entirely to physical oceanography.

As a contribution to the emerging understanding of the South Island west coast ecosystem, I have simulated the seasonal cycle of temperature and mixed layer depth by applying a vertical mixing model. A study area between 42 and 43°S was selected, this being the region for which the largest number of hydrographic stations was available. The near-shore zone is strongly influenced by run-off from the land, leading to a layer of less saline water at the surface. This layer moves along shore and is sometimes advected offshore (Stanton & Moore in press). To avoid this coastal influence, stations situated less than 70 km from the shore were excluded and the study area was delimited accordingly.

The study area is shown in Fig. 1. The figure also shows contours of sea surface temperature, as derived from NOAA satellite sensor data. These data were processed by the New Zealand Meteorological Service and such data are published in the form of weekly composite maps, as shown here for the week ending 4 May 1987. Calibrated temperatures are available from March 1984, and are accurate to 1°C. In contrast to the situation found east of the South Island, in the figure no sharp front between water masses of different temperatures can be discerned west of the South Island. Isotherms tend to be parallel to latitude circles in the open ocean, but usually bulge towards the south closer to the west coast. This leads to temperatures being c. 1°C warmer on the shelf than further offshore at the same latitude. It indicates a possible warming of the surface waters by southward advection, feeding into the Southland Current which flows around the southern tip of New Zealand.

A temperature section across the study area is shown in Fig. 2, and Fig. 3 displays a vertical temperature profile from Station V169 on this section. At this station the mixed layer is well-defined. Fig. 2

M91019
Received 1 May 1991; accepted 13 December 1991

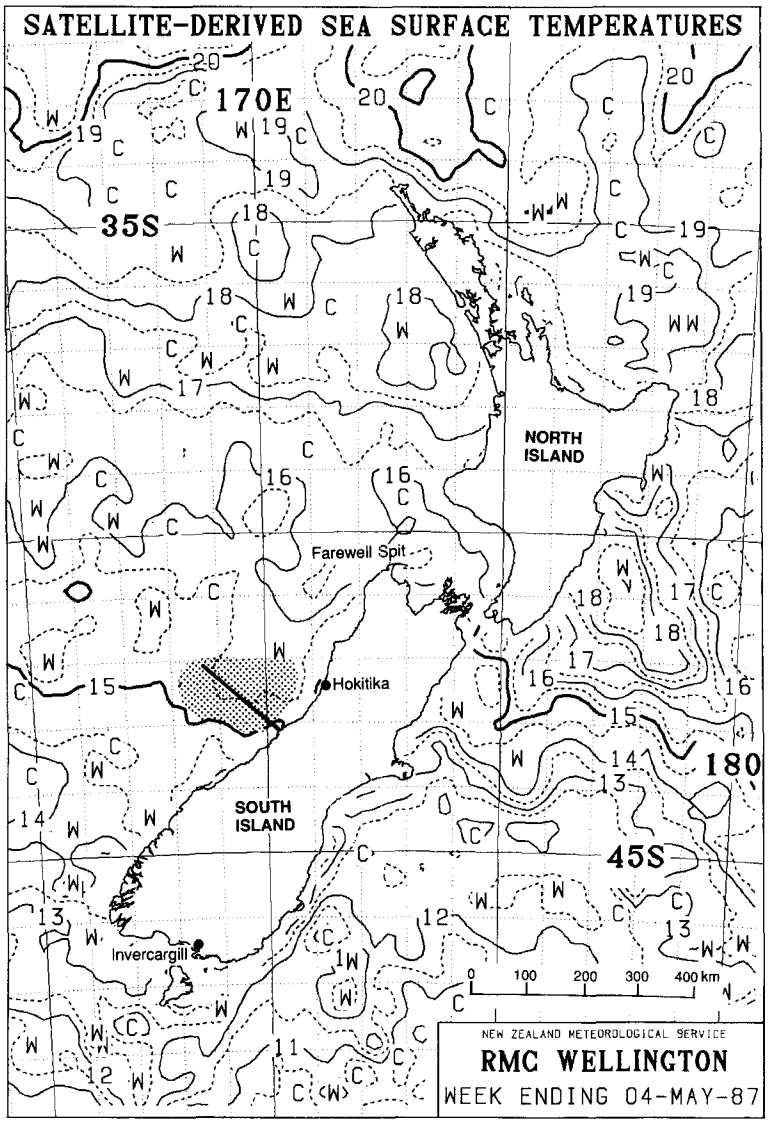

Fig. 1 Satellite-derived sea surface temperature around New Zealand for the week ending 4 May 1987. The study area is stippled. The straight line across the study area is the location of the temperature section shown in Fig. 2. The weather station locations at Invercargill, Hokitika, and Farewell Spit are also shown.

shows clearly that, away from the coastal boundary, the mixed layer is between 60 and 80 m deep, with a weak maximum of temperature and mixed layer depth near Station V170. The horizontal variability again indicates advective effects. Closer to the coast the boundary influence dominates. A temperature inversion at Station V173 is probably the result of offshore advection of colder water near the surface, associated with upwelling at the coast (Stanton & Moore in press). The one-dimensional mixing model used in this paper could not capture such coastal boundary effects, and was therefore only applied to a study area further offshore.

VERTICAL MIXING MODEL

The model used to calculate the temperature structure of the water column consists of an integrated mixed layer model for the surface layer, embedded into a simple advective-diffusive model for the thermocline. Fig. 4 presents a schematic view of the model. The time variation of the thermal structure is driven by meteorological forcing at the surface, using data of air temperature, cloud cover, humidity, solar radiation, and wind speed. From these data the four surface heat exchange terms are calculated with the help of parameterisation formulae: solar heating, long-wave

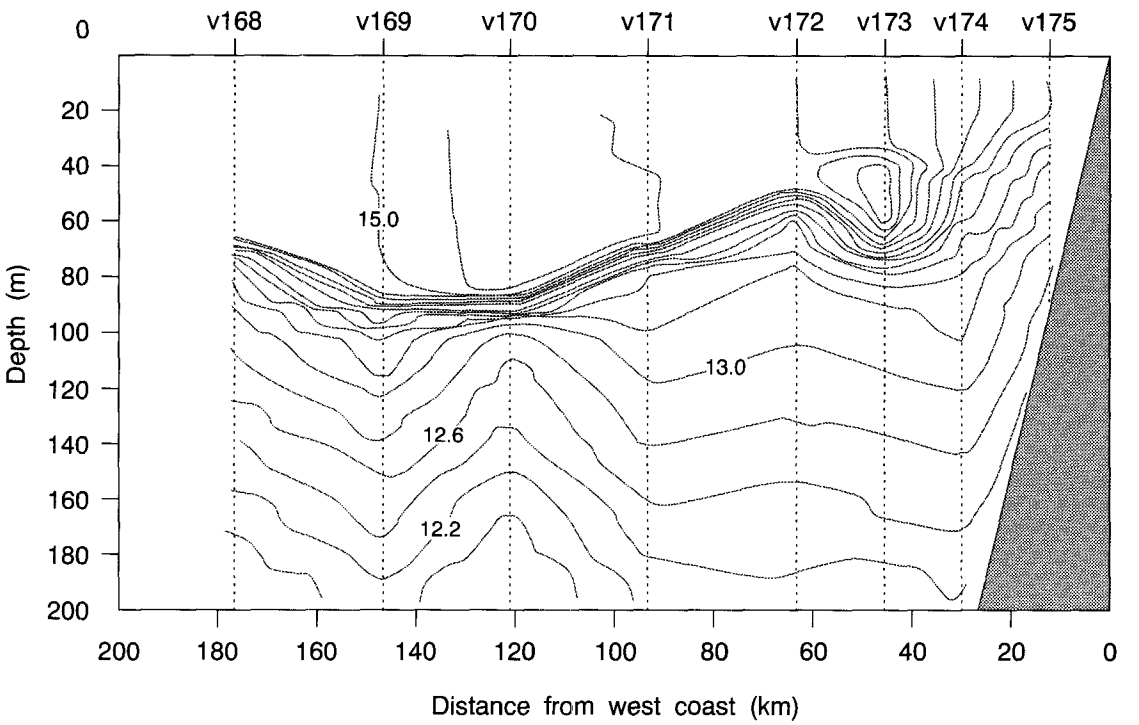

Fig. 2 Temperature section across the study area, as marked on Fig. 1. The data were collected on 28 and 29 April 1987 as part of the TASBEX I cruise. CTD stations are indicated by vertical dotted lines and are labelled with their station numbers.

back radiation, and sensible and latent heat exchange with the atmosphere.

At each time step, i.e., for each day, the distribution of this heat with depth is calculated as follows. The solar radiation is distributed according to an exponential depth dependency with two different length scales. The other heating (or cooling) terms act directly at the surface, i.e., at the uppermost level of the finite difference scheme, which has a vertical resolution of 2 m. After the heat input, the processes of convection and wind mixing are simulated with the mixed layer model. This calculates a new mixed layer depth and temperature according to the principles of heat and turbulent energy conservation, and is based on a similar, now classical model by Kraus & Turner (1967). The depth of convection is determined first, by mixing progressive levels starting from the top, until a statically stable water column is achieved. The potential energy released by this adjustment is calculated. This potential energy is converted to turbulent energy in the mixed layer, assuming that 12% of it can be used for further mixing, whereas 88% is lost to dissipation (Woods & Barkmann 1986).

The other source of turbulent energy for mixing is the wind. We assume that the wind power acting at the sea surface is proportional to the cube of the wind speed U. Again, most of this is dissipated, but a small fraction mU^3 can be used for mixing. The factor m is empirical, and is one of two crucial mixing parameters that need to be specified in this model. It is dependant on the mixed layer depth, as the wind stirring occurs near the surface and becomes less efficient for deeper mixed layers. Mixing a stably stratified water column requires work to be done against buoyancy forces, and the model determines the new mixed layer depth at each time-step by comparing this work to the available turbulent energy of penetrative convection and wind stirring combined.

Finally, vertical advection and diffusion below the mixed layer are simulated. Heat diffusion parameterises the mixing processes outside the turbulent mixed layer. It acts to smooth the temperature profiles and allows heat to penetrate below the mixed

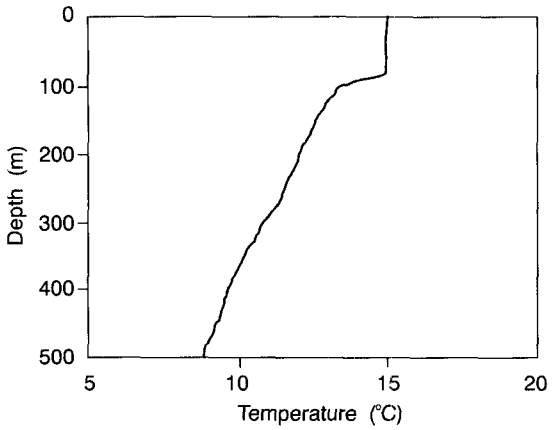

Fig. 3 Observed temperature profile at Station V169, which is part of the section shown in Fig. 2. The mixed layer is very clearly defined.

layer, both on a seasonal time scale and for longer-term climatic trends. The intensity of this process is specified by a turbulent diffusion constant K, which is the second important mixing parameter. The advection is small at 4 m/yr, and serves only to maintain a steady state thermocline for long-term calculations, i.e., several years. It does not represent any wind-driven upwelling events as can be observed further inshore along this coast.

This model for surface heating and mixing is published in Rahmstorf (1991). Full details can be found in Rahmstorf (1990). The model has been applied to zonal average climatology for a range of latitudes, and northern hemisphere observations of mixed layer depth (Tabata 1976) and temperature cycles (U.S. Navy 1981) were used to tune the model parameters. The best value found for the wind mixing efficiency is

$$m = 0.4 \times 10^{-3} \exp(-h/50m)\, \rho_a \kappa$$

where h is the mixed layer depth, ρ_a is the density of air (1.2 kg/m^3), and κ is the drag coefficient (0.0012). This choice of m is tuned to a time step of 1 day. More accurate calculations, which resolve the diurnal cycle, would need a somewhat larger value as a result of non-linear effects (Woods & Barkmann 1986). The value used for the turbulent diffusion constant is K = 1.0 cm^2/s. With these values, the model simulations agree well with the northern hemisphere data set for surface temperature and mixed layer depth (Rahmstorf, 1990). No parameters were tuned specifically for the South Island west coast model runs presented here.

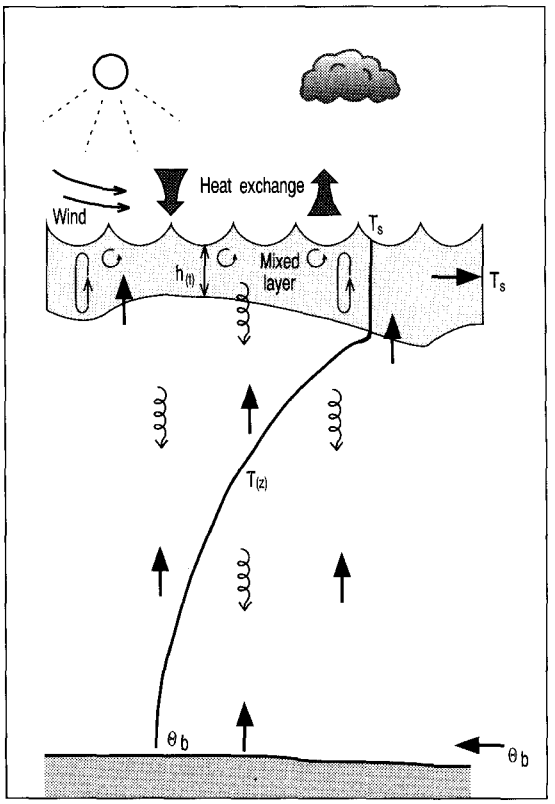

Fig. 4 Schematic representation of the vertical mixing model used in this work. A mixed layer (shaded) of variable depth $h(t)$ overlies an advective-diffusive deep ocean. The mixed layer is heated by solar radiation, exchanges heat with the atmosphere, and is stirred by the wind. Circles and ellipses in the mixed layer denote wind mixing and convection. The heavy arrows show advection, and the coiled arrows turbulent diffusion of heat.

METEOROLOGICAL DATA

A problem in modelling ocean conditions is finding suitable weather data to drive the simulations. Weather observations in the study area are sporadic, and a decision had to be taken as to which coastal weather station best represents conditions at sea. Some experimental work at sea was performed for the purpose during a cruise of RV *Rapuhia* to the South Island west coast in July/August 1988. The results were primarily used to correlate wind observations at sea with those from coastal stations, which will be the subject of the next Section. In this Section we look at the other weather parameters. Of the weather stations on the west coast of the South Island, Farewell Spit lighthouse was most representative of ocean

conditions. It is located on a low sand spit on the north-west corner of the South Island (Fig. 1). It is exposed to weather from the sea from all directions except the south. The weather stations in Hokitika and Haast are closer to the study area, but are backed by the snow-topped Southern Alps. These set up local weather patterns that are rather different from those encountered at sea. For example, cold katabatic winds frequently descend from the mountains, leading to offshore flow and relatively low temperatures at these stations. The alps also have a strong effect on cloud formation, and they disturb the wind, particularly in northwesterly flows.

The data set obtained for Farewell Spit extends from 1972 to mid 1989. However, an automatic weather station (AWS) replaced the manual observations by the lighthouse keeper during this time. Both types of data, manual and automatic, were collected in parallel from 1 January 1980 until 22 June 1984. The end of observations by the lighthouse keeper was unfortunate, because it meant that no cloud cover observations were available after June 1984, which is the time period of most interest for this work. I have therefore assumed that cloud cover acts essentially as a random forcing with no significant trends and interannual variation. The seasonal signal in the available cloud cover data is negligible, and shows little interannual variation (Rahmstorf 1990). This justifies the use of cloud cover values of corresponding days of 1975 as a rough approximation of the missing data after June 1984, where the year 1975 was selected at random. A single year was preferred to the use of a climatological average, because the average has rather different statistical properties, while having nearly the same mean as any individual year.

Another difficulty arose from the humidity data. The AWS humidities are much lower than those collected manually at the same time. Whereas AWS values centre around 60% relative humidity, the manual observations are generally around 80%. In test runs with the model, the AWS humidities led to sea surface temperatures c. 2°C cooler than those using the manual humidities (with all other data remaining the same). This is because low humidity in the air overlying the ocean leads to enhanced evaporation and therefore cooling. Comparison with our shipboard observations during the 1988 cruise showed that the humidity values at sea are generally around 80%. I therefore used the manual observations from Farewell Spit where available, and used 1975 manual humidity values after June 1984.

The air temperatures also differ between the manual and AWS data by sometimes more than 1°C, but the differences were random errors and there was no significant trend. Manual temperature data were used up to 31 December 1979, and AWS data afterwards. Clear sky solar radiation was derived from a theoretical formula given by Henderson-Sellers (1986), for 42°30'S. From the discussion above, it is clear that the quality of the meteorological data severely limits the accuracy with which we can determine the surface heat exchange in the ocean area under study.

WEST COAST WIND CORRELATIONS

A parameter of prime importance in the mixing model is the wind speed. Wind speeds on the open sea are likely to be different from those at the coast. For this reason, the wind speed observations made during the 1988 cruise were used to analyse the correlation between wind speeds measured at sea and at nearby coastal stations. A new method was used for the wind measurements at sea, to reduce disturbance caused by the ship and to improve the accuracy (Rahmstorf 1989). The aim was to determine which coastal station would be most representative of the wind speed at sea off the South Island west coast.

Only one comparable study has been published for the area. Neale & Thompson (1978) compared fairly regular reports from two fishing vessels over 12 months with coastal observations from Haast and Hokitika. They distinguished two major weather patterns: broad-scale southwesterly flows and broad-scale northwesterly flows. In the former situation, wind blows parallel to the mountain range and is well confined to directions between 180 and 270°, i.e., the southwest quadrant. In the latter situation, ground-level winds are disturbed by the mountains and can come from any direction between 270 and 180°, i.e. the remaining three quadrants.

Neale & Thompson (1978) found that wind speeds at Haast and Hokitika were very similar, but differed from those at sea. In stronger winds, the speed at the coast was much lower than at sea, and was not well correlated. In low wind situations, the coastal stations showed marked diurnal variations as a result of katabatic winds, which were absent at sea. Below about 4 knots, winds were on average stronger at the coast than at sea. These results indicate that the wind at Hokitika is a poor predictor of winds further offshore.

Unpublished work by Basil Stanton (pers. comm.) confirms this conclusion and indicates that Farewell Spit winds might be better correlated to conditions in the open sea off the South Island west coast. As a further option, I examined 900 mb balloon winds

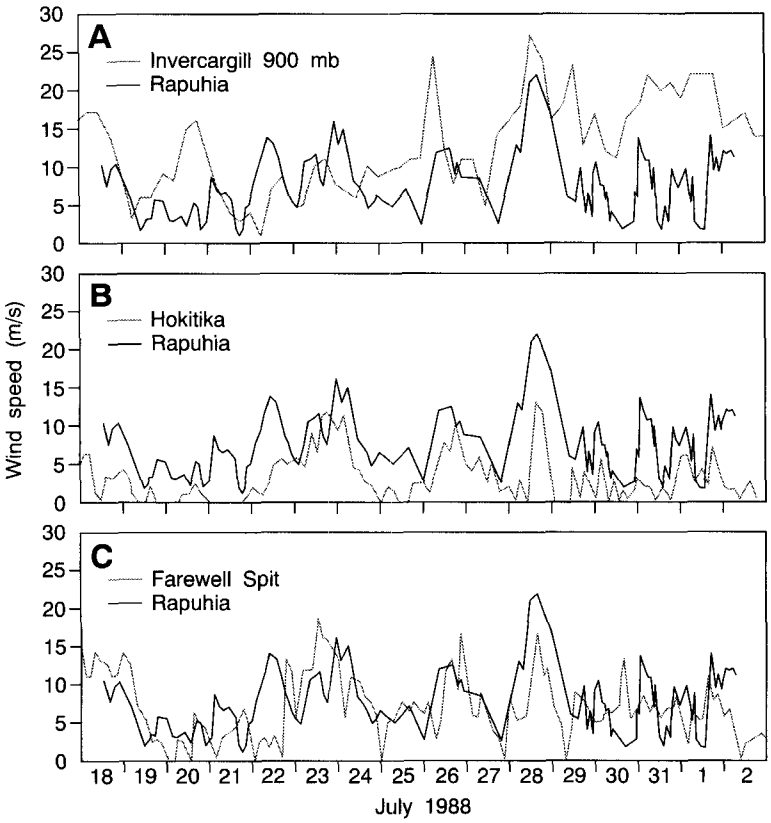

Fig. 5 Observed wind speed at: A, Invercargill at the 900 mb level; B, at Hokitika Airport; and C, at Farewell Spit Lighthouse. These are compared to shipboard measurements from RV *Rapuhia*.

from Invercargill. Like Farewell Spit winds, they should be little affected by the mountain range.

Wind time series from Farewell Spit, Hokitika and Invercargill were compared to the measurements from RV *Rapuhia* taken during the winter 1988 cruise. The time series are shown in Fig. 5. Weather maps showed that the observation period included times of broad-scale northwesterly flow from 23 to 27 July and southwesterly flow from 18 to 23 and from 27 to 31 July. The shipboard measurements were taken from a boom off the side of the ship, with the ship aligned parallel to the wind. They are described in more detail in Rahmstorf (1989). After visual inspection the Invercargill winds were rejected, because they show several periods of very strong winds which are not matched by similar events at sea.

Further analysis was restricted to Farewell Spit and Hokitika. Because of the irregular data spacing, 6-h averages of wind velocity were calculated for these stations as well as RV *Rapuhia*, to obtain simultaneous data points for comparison. For the coastal stations, the mean direction was also calculated, by averaging vectors. *Rapuhia* wind speed was plotted versus coastal wind speed, with different symbols for wind directions from the four quadrants. This revealed that winds from the southwest quadrant had a distribution different to that of the other directions. The data set was therefore split into two groups: winds from between 180 and 270° (inclusive), and others. For both groups, a linear least squares fit as well as an integral fit was calculated. The latter is obtained by dividing the total wind run of the observation period for the coastal stations by that for the ship. This measure has the advantage that it does not rely on the 6-h averages, but integrates the original data set.

In all measures the Farewell Spit winds were clearly better correlated than the Hokitika winds. If we multiply the coastal winds by a factor A to obtain the wind at sea, then the best estimate for this factor is 1.63 for southwest winds and 0.94 for other directions if the Farewell Spit winds are used. For Hokitika winds, the conversion factors would be 2.9 and 2.5 respectively: winds at Hokitika are much weaker than at sea. These estimates of A were derived with the integral criterion, though the results of the least

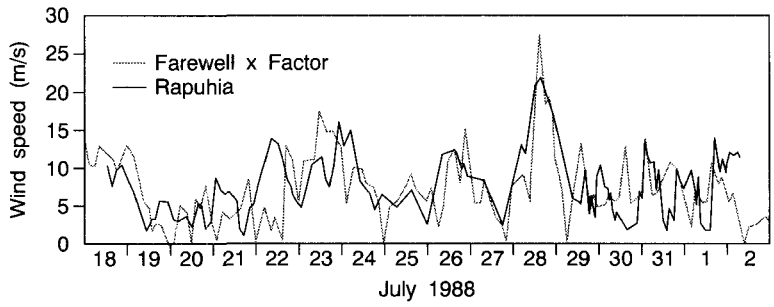

Fig. 6 Corrected wind time series from Farewell Spit, compared to the wind speed observed from RV *Rapuhia*. The correction factor was 1.63 for south-westerly winds, and 0.94 for other directions.

squares fit are very similar. If we use the whole data set without distinguishing wind directions, the conversion factor would be 1.2 for Farewell Spit and 2.6 for Hokitika.

For the model, we are also interested in the cube of the wind speed, as this determines the energy available for mixing. With the same factor A derived above for the speed, we also get the correct integral of the cube of the wind speed within 3% for Farewell Spit. For Hokitika, the wind cubed estimate would be 40% too high, and we would have to apply different conversion factors depending on whether we want to calculate wind speed, wind stress, or cube of the wind speed. This indicates that the wind statistics at Farewell Spit resemble those at sea, whereas those at Hokitika do not.

The time series obtained by multiplying the coastal wind speed by A was compared to the speed actually observed at sea. The difference between the derived wind and the observed wind can be expressed as a root mean square (RMS) error. For Hokitika, it is 6.0 m/s, whether or not one differentiates between different wind directions. For Farewell Spit, the RMS error is 4.5 m/s if we use $A = 1.2$ for the whole time series. It improves to 4.0 m/s if we use $A = 1.63$ for southwesterly winds and $A = 0.94$ for other directions. The time series obtained in this way is shown in Fig. 6. This method was used to derive wind speed estimates for the model runs. The time series that was available to derive the conversion factors is short, but included the classical sequence of alternating northwesterly and southwesterly flows which prevails in the area throughout the year.

MODEL SIMULATIONS FOR THE WEST COAST

The meteorological data set for air temperature, humidity, cloud cover, solar radiation, and wind speed, described in the previous sections, was used to drive the vertical mixing model. The simulation was started on 1 January 1973 with an exponential temperature profile

$$T(z) = T_d + (T_0 - T_d)e^{z/788m},$$

with $T_0 = 14.4°C$ and $T_d = 1.1°C$. The depth z is measured positively upwards. The length scale of 788 m for the equilibrium profile is determined by the balance of diffusion and upwelling (with velocity $w = 4$ m/yr) as K/w. The best parameter T_0 for the initial profile was found by trial and error. It minimises the net heat content change of the upper layer and the deep ocean in the first few years of the simulation, thereby showing that this profile is close to the equilibrium profile. T_d is determined by the temperature of the bottom water that enters the model at its lower boundary. The starting date was suitable because at that time of the year the mixed layer is shallow, and deviations from the exponential profile are confined to a thin surface layer.

I show the results for 1979–89, because there are some observations for comparison for this period. The calculated sea surface temperatures are shown in Fig. 7 and compared to shipboard observations. These observations were collected by the New Zealand Oceanographic Institute. They were compiled from published results (Bradford 1983; Heath & Ridgway 1985; Bradford & Chang 1987) and from internal data reports for the TASBEX I (November 1986), TASBEX II (May 1987), Mintrex I (July 1987), Hoki I (July 1987), 2021 (July 1988), and Mintrex III (February 1989) cruises. All observed temperatures are fairly close to the simulated curve. To describe the characteristics of the temperature cycle produced by the model, a least square fit sinusoidal cycle was matched to the output data of Fig. 7. This showed that the average seasonal cycle (for 1979–88) has an amplitude of 3.0°C with a mean temperature of 15.2°C. The maximum mixed layer temperature was reached on 18 February and thus lagged the solar forcing cycle by 60 days.

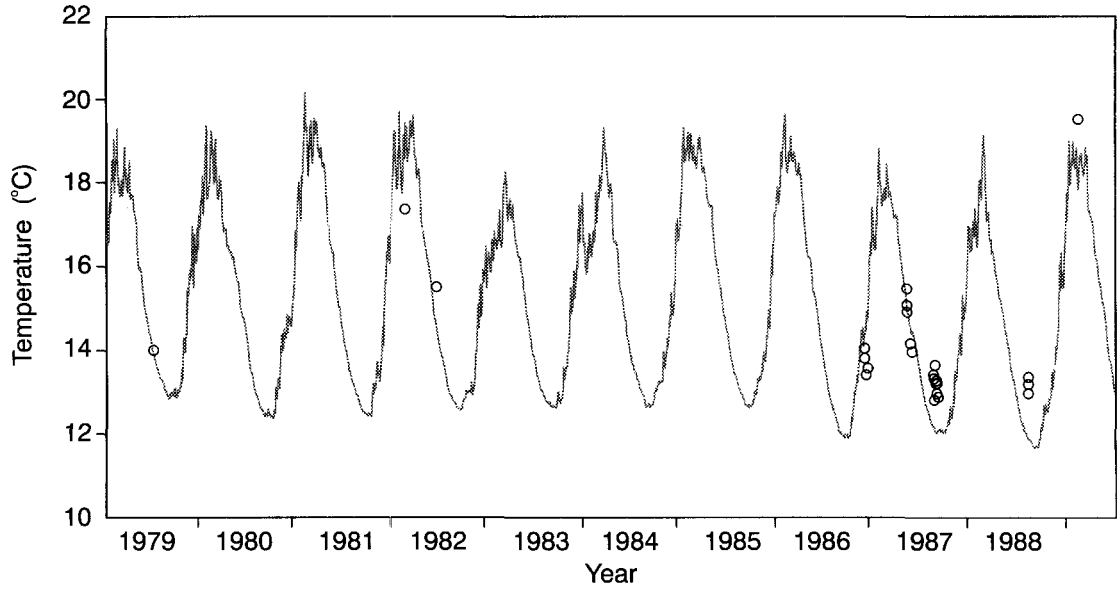

Fig. 7 Modelled sea surface temperature in the study area off Westland, and shipboard observations (circles).

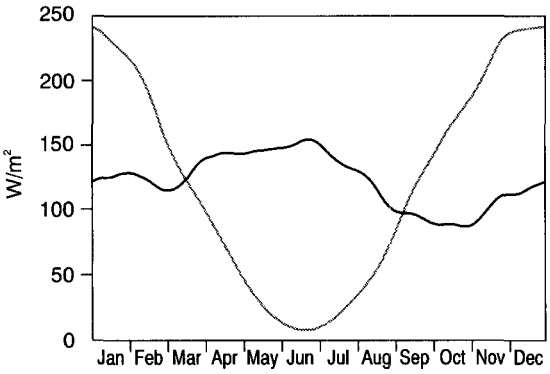

Fig. 8 Average annual cycle of the ocean-atmosphere heat flux and the radiation balance in the model. The dashed line is the radiation budget at the sea surface, i.e. incoming solar radiation minus outgoing long-wave back radiation. The solid line is the heat transferred to the atmosphere, i.e. the sum of the sensible and latent heat fluxes. The curves are 10-year averages of daily values, low-pass filtered with a cosine bell filter of 51 days total width.

For comparison, the air temperature observations used to drive the model were analysed in the same way. They showed a stronger seasonal cycle with an amplitude of 4.1°C and a cooler average temperature of 13.4°C, consistent with a mean flow of heat from the ocean to the atmosphere. Air temperature lagged the solar forcing by 35 days, reaching its maximum on 25 January. The average heating rate of the ocean by the sun was 186 W/m^2. This was balanced by back radiation (64 W/m^2) and transfer of heat to the atmosphere in the form of latent heat (107 W/m^2) and sensible heat (16 W/m^2). Fig. 8 compares the seasonal cycle of the radiation budget at the sea surface with the ocean-atmosphere heat flux. In the long term these two components balance, but their seasonal behaviour differs markedly. In spring and summer the radiative heating from the sun is strong and exceeds the heat loss to the atmosphere, so that the ocean warms up and stores heat. At the beginning of winter the radiative heating reaches a minimum where long-wave back radiation almost equals the incoming short-wave radiation. Around the same time the air-sea heat flow reaches a (weak) maximum, so that the ocean cools rapidly and the mixed layer deepens through convection. The graph illustrates how the oceanic mixed layer acts as a heat buffer: it ameliorates the seasonal heating cycle of the sun by storing heat and releasing it to the atmosphere at a relatively constant rate year-round.

The simulated mixed layer depths are shown in Fig. 9. For the model, I plotted the weekly maxima of mixed layer depth. This substantially reduces the daily fluctuations, which result from the very shallow mixing depths on calm days. Weekly maxima are

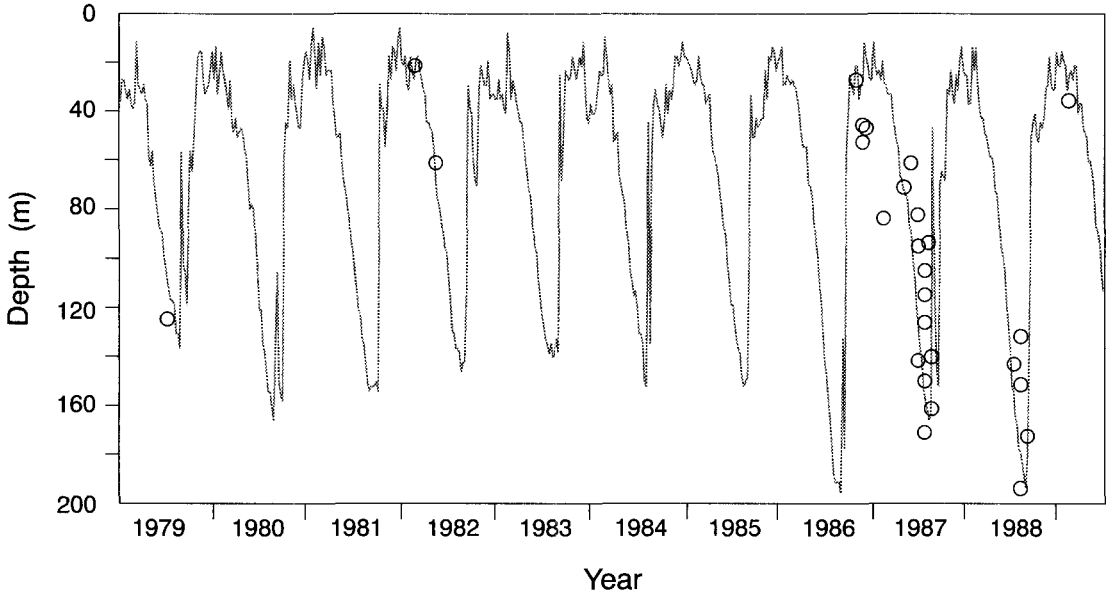

Fig. 9 Modelled mixed layer depth in the study area off Westland, and shipboard observations (circles).

also more suited to comparison with observed mixed layer depths, which I derived from temperature profiles (Fig. 3) by visual inspection. Even after mixing has ceased, the last maximum depth of mixing will be the one visible in the profile for some time, until the water is noticeably warmed and a new temperature step forms, while the old one is eroded by diffusion. The modelled curve agrees well with observations. The annual range of mixed layer depth, from up to 200 m in winter to between 10 and 40 m in summer, seems to be modelled well. The large interannual variability of the deepest winter mixing is interesting: the calculated mixed layer depth reached 195 m in 1986, but only 152 m in the year before. Unfortunately the observations are not sufficient to determine how well these predictions represent the real ocean.

Some of the measured interannual variability of coastal temperatures around New Zealand is related to the El Niño / Southern Oscillation phenomenon (Greig et al. 1988), and it is interesting to see whether the modelled mixed layer cycles also show such a teleconnection. A link could occur through the surface forcing, if the weather data from Farewell Spit are correlated with the Southern Oscillation. Three El Niño events occurred during the time span we modelled, with corresponding minima in the Southern Oscillation Index in 1976, 1982–83, and 1987 (Enfield 1989). The three coldest summers in the modelled sea surface temperatures off Westland were 1975/76 (not shown in Fig. 7), 1982/83, and 1986/87. This is consistent with the results of Greig et al. (1988), who found that El Niño years were characterised by cooler sea surface temperatures at Leigh and Portobello (on the east coast of the North Island and South Island respectively). The cooler temperatures seem to have no obvious effect on the mixing depths. In summer, the modelled mixed layer depths showed little interannual variability. In winter, in 1982 the depth of mixing was comparatively shallow, whereas 1976 and 1987 had rather deep winter mixed layers. Apart from the direct weather forcing, the winter mixing depth also depends on past temperature history, which is "remembered" in the water column over the remainder of the year, whereas the deep waters are virtually decoupled from the surface forcing. Advection also plays an important role at these depths, as I will discuss below.

Rahmstorf (1991) studied the sensitivity of the mixing depth to changes in climate. A warming of the sea surface by 2°C would lead to a decrease in the depth of winter convection by about 15 m at this latitude, whereas during the remainder of the year the mixed layer depth would be hardly affected. An increase or decrease in wind speeds, associated with climatic change, would increase or decrease the mixed

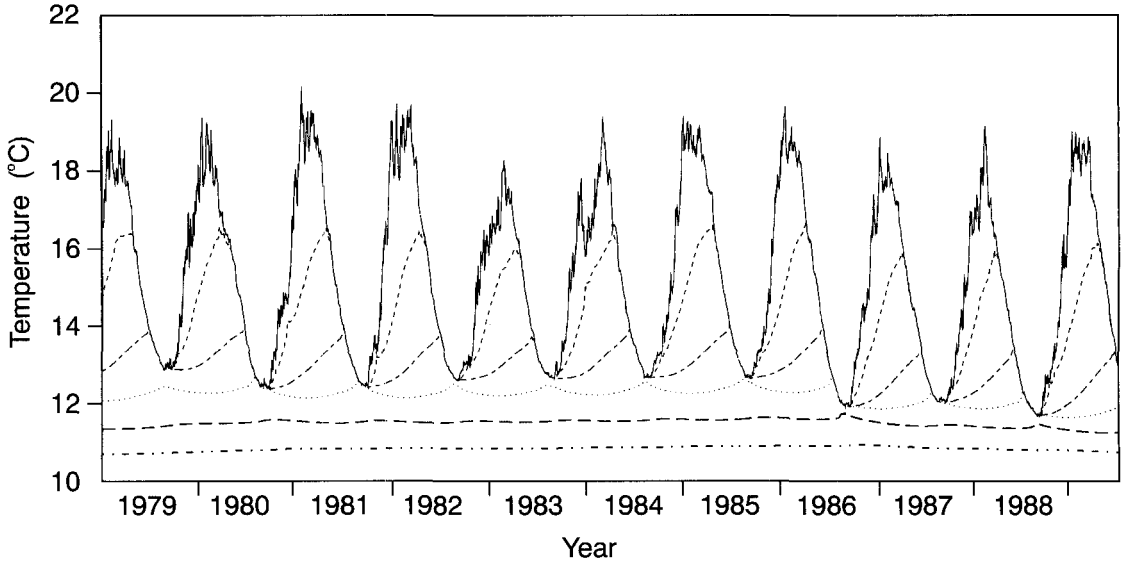

Fig. 10 Modelled ocean temperature at different depths: at the surface (uppermost curve); 50 m (dashed curve); 100 m (dotted); 150 m (dash-dotted); 200 m (line); and 250 m (bottom curve).

layer depth throughout the year, but most notably in summer.

Fig. 10 shows how the seasonal heating signal penetrates below the surface waters of the ocean in the model. With increasing depth the maximum temperature gets cooler and is reached later in the year, namely when the corresponding water is engulfed by the deepening mixed layer in autumn or early winter. The maximum temperature at a given depth is therefore equal to the surface temperature at the time when the mixed layer reaches this depth. At 50 m depth this occurs in the first half of March, at 100 m around mid June, and at 150 m in mid or late July. Near the deepest mixing depth, therefore, the seasonal cycle is practically reversed, with warmer temperatures in winter and cooler temperatures in summer. The water below the depth of winter mixing is practically unaffected by the seasonal cycle.

Only limited data are available to test these predictions for the subsurface temperatures off the West Coast. Garner (1969) noted that bottom temperatures at mid-shelf (at c. 120–140 m depth) are warmer in winter than in summer, and he concluded that advection must be the reason. The model shows that we can expect warmer winter temperatures at this depth as a result of the delayed vertical penetration of the seasonal heating signal alone. However, because this seasonal signal gets weaker with increasing depth, it is likely that horizontal advection can dominate the temperature variability in deeper waters. Some useful information about this can be derived from the temperature records from the TASBEX moorings (Stanton & Moore in press). However, only one of these moorings was situated within the study area for this paper (Mooring B, 100 m below surface). Mooring D was accidentally displaced by a trawler and recovered 1 year later. Although its exact location is therefore unknown, it was inshore of the study area at c. 50 m depth. Moorings E, F, and G were located north of the study area on a line off Farewell Spit, and recorded at 100, 70, and 50 m below surface respectively. In spite of the geographical spread of these moorings I plotted these temperature time series together with the model predictions (Fig. 11). At these depths rapid temperature changes occurred of the same magnitude as the expected seasonal signal caused by vertical mixing. These changes are correlated with the measured currents and are therefore most likely caused by advection (Stanton pers. comm.). In times of southward flow the temperatures increase, and in northward flow they drop. An important part of the variation in currents (and thus temperature) in this area is caused by propagating coastal-trapped waves, caused by wind forcing in Cook Strait (Cahill et al. 1991).

Better time coverage than by the ship or mooring data is achieved by satellite observations which are compared with the model results in Fig. 12. They are, of course, restricted to sea surface temperature. The

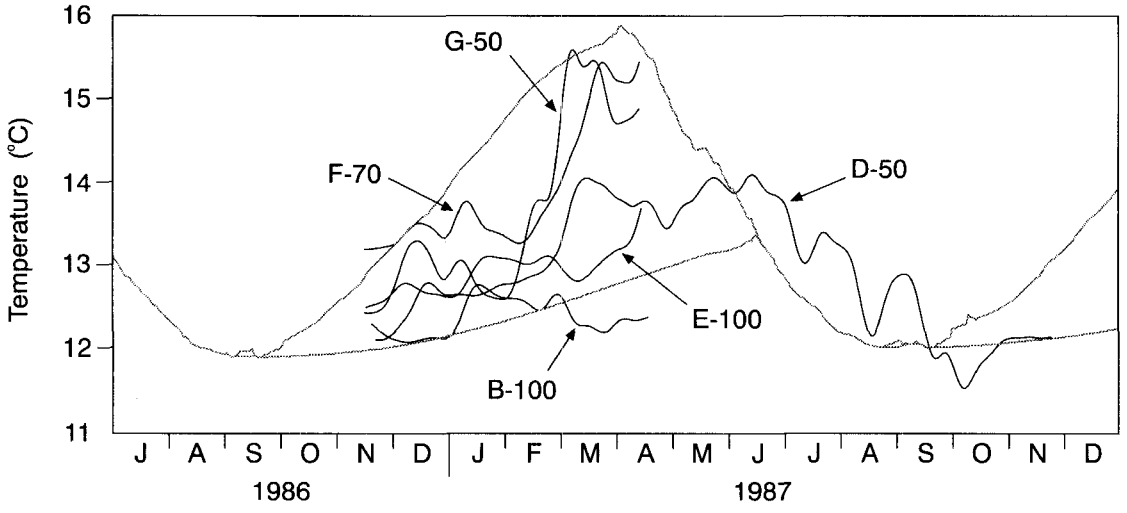

Fig. 11 Modelled ocean temperature at 50 (upper dotted line) and 100 m depth (lower dotted line), compared to time series from various moored instruments (low pass filtered). A capital letter denotes the mooring name, followed by a number which gives the depth of the temperature recorder.

Fig. 12 Sea surface temperature off Westland, as calculated by the model (dotted line) and derived from satellite pictures (solid line).

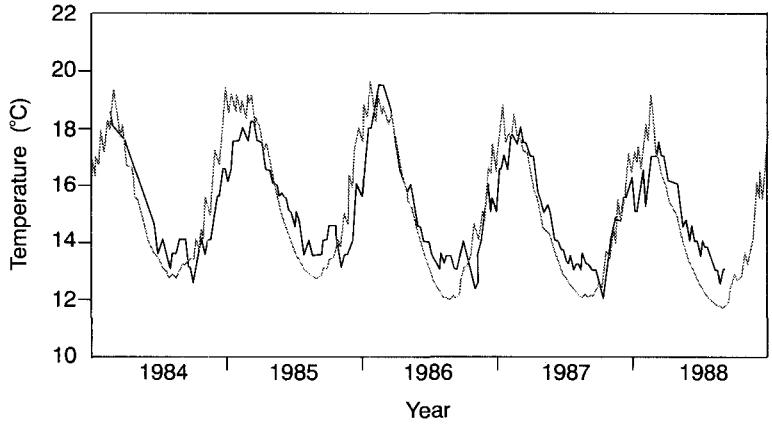

figure shows that the seasonal temperature cycle, ranging from 12–13°C in winter to 18–20°C in summer, is simulated quite well by the model, but there is a small phase difference between model and satellite observations. The phase difference could result from the fact that the satellite data in a certain location are only refreshed when there is no cloud covering this location, so that the satellite will see changes in the ocean only some time after they occur. In spite of the phase difference, the RMS difference between the two time series is only 1.2°C. If the modelled time series is lagged by 2weeks to improve the match with the satellite data, the RMS difference drops below 1.0°C.

EFFECTS OF HORIZONTAL ADVECTION

In the mooring time series (Fig. 11), we have already seen how the effects of advection are superimposed on the heating by vertical mixing. There is also some evidence for advection in the satellite observations of surface temperature. If we subtract the (model's) average seasonal cycle from both curves in Fig. 12, we arrive at the curves of Fig. 13. This graph emphasises deviations from the average cycle, such as particularly warm or cold periods. Clearly, such deviations are not well correlated between model and satellite observations. The observations show consistent warm deviations from the model's cycle

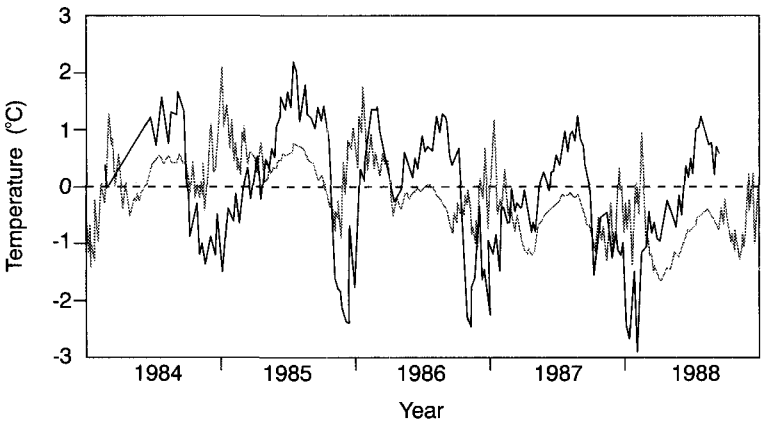

Fig. 13 Modelled and satellite-derived sea surface temperature as in Fig. 12, but with the average seasonal cycle removed.

during winter. This may be caused by horizontal advection of warmer water into the study area. Fig. 12 supports this speculation. Although the model goes through smooth winter minima, the observations show spiky warm events. These cannot be explained by surface heating alone, as the model results show. Temperature fluctuations resulting from the variability of the surface forcing are very small in winter, because of the large heat capacity of the deep mixed layer. In the observations, in contrast, short-period fluctuations are of similar magnitude throughout the year, indicating that they have other reasons than surface heating. It is quite possible, however, that they are caused by measurement errors in the satellite-derived sea surface temperatures. Heath & Ridgway (1985) describe temperature fluctuations with periodicities of 1–4 and 6 weeks off this coast, which they attribute to horizontal exchange.

If the differences between modelled and observed temperatures are the result of horizontal advection, then the model could in principle be used to obtain estimates of this advection. Recently, Elliott & Clarke (1991) used a similar model in the North Sea, and were able to derive realistic residual currents by an inverse method based on the differences between observations and their model results. Horizontal advection accounted for differences of 2°C in the northern North Sea. However, such investigations can only be successful if we have faith in the accuracy of the surface heat flux driving the model as well as the observed sea surface temperatures. We did not have sufficient available data. An observation programme with thermistor chain moorings and meteorological buoys would allow a more detailed analysis of the temperature variations off the West Coast and their causes.

A look at the shape of the isotherms in the area, as seen from satellite, can give us a qualitative idea of the large-scale effects of horizontal flow on the surface temperatures. Fig. 14 shows a selection of isotherms that is typical for the sea surface temperatures off the South Island west coast. Shown are 13°C isotherms in September for the years 1985–89. They bulge southward over the shelf off the coast, and swing back to the north further inshore. This is consistent with a flow regime where water approaches the South Island from the west and turns southward over the flank of the Challenger Plateau, flowing into the Southland Current around the southern tip of New Zealand. Further inshore, there is a northward going coastal current, and/or upwelling of colder water. This view broadly agrees with geostrophic currents derived from the TASBEX experiment (Stanton & Moore in press), and earlier data (Stanton 1976; Stanton & Richman in press), although the currents in the region are complex and highly variable. The geostrophic adjustment of the mixed layer to this flow pattern would result in a mixed layer depth maximum roughly parallel to the coast, located between the southward and the northward flow. Such a maximum was observed during cruises in April 1974 and June 1979, and from these data Heath (1984) concluded that the mixed layer topography is closely linked to the geostrophic flow. This maximum is also evident in the TASBEX data set (November 1986 and May 1987), and is visible in Fig. 2 at 120–140 km off the coast.

Though only isotherms for September are shown in Fig. 14, they are representative of the situation all year round; the southward displacement is a permanent feature which is visible in most (but not all) of the sea surface temperature charts. It was first noted by Heath

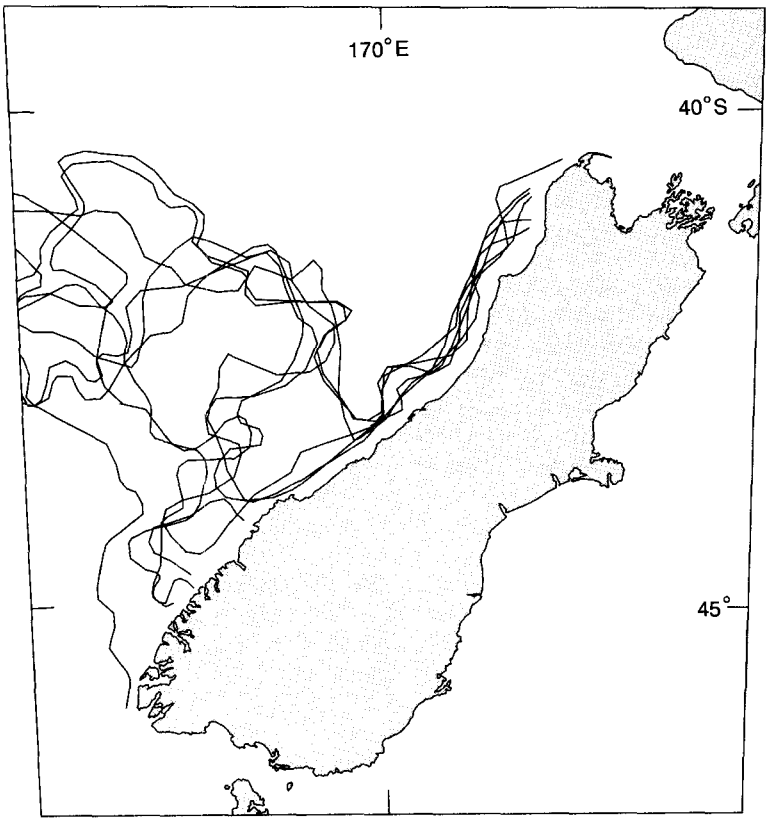

Fig. 14 A selection of 13°C isotherms for September of years 1985–89.

& Ridgway (1985) on a satellite photograph from 12 June 1982. We can make a rough estimate of the southward heat transport that is associated with the southward displacement of the isotherms, by assuming that it is in thermodynamic balance with the surface heat exchange. At a given location in the ocean, the advective heating rate (per unit area) resulting from a southward flow past this location is

$$Q_{ad} = V c_p \rho \partial T/\partial y ,$$

where V is the volume transport per unit width, c_p is the specific heat of sea water, ρ its density, and $\partial T/\partial y$ is the meridional temperature gradient. The temperature increase caused by this heating rate is

$$\Delta T = Q_{ad}\, \partial T/\partial Q ,$$

and this leads to a southward displacement of an isotherm by

$$\Delta y = \frac{\Delta T}{\partial T / \partial y}.$$

Combining these three equations, we obtain an expression relating the transport to the isotherm displacement, which is independent of the actual north-south temperature gradient:

$$V = \frac{\Delta y}{c_p \rho \partial T / \partial Q}.$$

The key parameter is the temperature sensitivity $\partial T/\partial Q$, which we can work out from the heat flux parameterisations used in the model calculations. If we assume that the atmospheric parameters such as air temperature remain constant, then these formulae show that an increase in sea surface temperature by 1°C leads to an increase in back radiation of 1.0 W/m^2, an increase in sensible heat loss of 11.4 W/m^2, and an increase in evaporation of 27.4 W/m^2. This means that an advective heating rate of 40 W/m^2 would lead to an equilibrium warming of 1°C, so that the temperature sensitivity value is 0.025 K/(Wm^{-2}). This sensitivity value depends on temperature, wind speed, and relative humidity, and the figure given is characteristic for South Island west coast conditions. The volume transport (per unit width of current) required to shift isotherms southward by 2° latitude is

then c. 3 m^2/s. For a current throughout the mixed layer this would imply a velocity of 3 cm/s if the mixed layer is 100 m thick, or 6 cm/s if the mixed layer is 50 m thick. These values are comparable to the geostrophic current velocities reported for this area by Stanton & Moore (in press), but are only a rough estimate. If we estimate the total transport by integrating across the width of the southward bulge in the surface isotherms, we obtain a value of 0.4 Sv. This is smaller than the geostrophic transport measured during the TASBEX experiment across the Heretaniwha line, which was 0.8 Sv (Stanton & Moore in press). It is clear from these calculations that the currents observed in the region are strong enough to explain the tongue of warm water that stretches southward over the West Coast shelf.

CONCLUSIONS

The success of the vertical mixing model shows that the seasonal variation in mixed layer depth and temperature can be explained in its basic features by the solar forcing and local air-sea heat exchange. The summer mixed layer depth of around 20 m is largely determined by a balance between heating and wind mixing, whereas in winter the mixing depth (140–200 m) depends more on convection than on the wind. The average sea surface temperature is 15.2°C, and the amplitude of the seasonal variation is 3.0°C. This variation dies down with depth and virtually disappears at 200 m. The temperature maximum is reached in February at the surface, and progressively later further down, so that at 150 m depth the seasonal cycle is reversed. Fluctuations in surface temperature and mixing depth associated with spells of particularly sunny or windy weather, for example, can in principle be predicted by the model, but the available weather data for the South Island west coast are not sufficient for this.

Superimposed on the variability caused by the local forcing are the effects of advection. They can lead to short-term temperature variations associated with coastal-trapped waves or other transient currents. Below the surface, where the atmospheric forcing is weak, these advective effects can dominate the temperature signal. In addition to these short-term variations, there is also a persistent warming associated with the southward transport of warm water into the study area throughout the year. This warmer water does not reach the coast. The geostrophic adjustment to this flow will modulate the mixed layer depth, and probably explains the maximum in mixed layer depth that is observed running roughly parallel to the coast.

Some uncertainties remain, however, about the interpretation of the South Island west coast mixed layer dynamics presented in this paper. A main cause of this uncertainty is that too little is known about the prime driving force, the weather at sea.

ACKNOWLEDGMENTS

Thanks are expressed to all who participated in Cruise 2021 and helped with the collection of meteorological data around the clock. I am grateful to the New Zealand Meteorological Service, in particular to Andrew Laing, for support and the provision of weather data. Basil Stanton, Tim Shirtcliffe, Mike Moore, and Rob Murdoch contributed with helpful comments during various stages of this work.

REFERENCES

Bradford, J. M. 1983: Physical and chemical oceanographic observations off Westland, New Zealand, June 1979. *New Zealand journal of marine and freshwater research 17*: 71–81.

Bradford, J. M.; Chang, F. H. 1987: Standing stocks and productivity of phytoplankton off Westland, New Zealand, February 1982. *New Zealand journal of marine and freshwater research 21*: 71–90.

Cahill, M. L.; Middleton, J. H.; Stanton, B. R. 1991: Coastal-trapped waves on the west coast of South Island, New Zealand. *Journal of physical oceanography 21*: 541–557.

Elliott, A. J.; Clarke, T. 1991: Seasonal stratification in the north west European shelf seas. *Continental shelf research 11*: 467–492.

Enfield, D. B. 1989: El Niño, past and present. *Reviews of geophysics 27*: 159–187.

Garner, D. M. 1969: The seasonal range of sea temperature on the New Zealand shelf. *New Zealand journal of marine and freshwater research 3*: 201–208.

Greig, M. J.; Ridgway, N. M.; Shakespeare, B. S. 1988: Sea surface temperature variations at coastal sites around New Zealand. *New Zealand journal of marine and freshwater research 22*: 391–400.

Heath, R. A. 1984: The depth of the mixed layer as an indicator of oceanic circulation around New Zealand. *New Zealand journal of marine and freshwater research 18*: 83–92.

Heath, R. A.; Ridgway, N. M. 1985: Variability of the oceanic temperature and salinity fields on the West Coast continental shelf, South Island, New Zealand. *New Zealand journal of marine and freshwater research 19*: 233–245.

Henderson-Sellers, B. 1986: Calculating the surface energy balance for lake and reservoir modeling: a review. *Reviews of geophysics 24*: 625–649.

Kraus, E. B.; Turner, J. S. 1967: A one-dimensional model of the seasonal thermocline. II. The general theory and its consequences. *Tellus 19*: 98–105.

Neale, A. A.; Thompson, G. M. 1978: Surface winds in coastal waters off Westland. Wellington, New Zealand Meteorological Service.

Rahmstorf, S. 1989: Improving the accuracy of wind speed observations from ships. *Deep sea research 36*: 1267–1276.

———1990: An oceanic mixing model: application to global climate and to the New Zealand west coast. Unpublished PhD thesis, Victoria University of Wellington, New Zealand. 169 p.

———1991: A zonal-averaged model of the ocean's response to climatic change. *Journal of geophysical research 96*: 6951–6963.

Stanton, B. R. 1976: Circulation and hydrology off the west coast of the South Island, New Zealand. *New Zealand journal of marine and freshwater research 10*: 445–467.

Stanton, B. R.; Moore, M. I. in press: Hydrographic observations during the Tasman boundary experiment off the west coast of South Island, New Zealand. *New Zealand journal of marine and freshwater research.*

Stanton, B. R.; Richman, J. G. in press: Density driven currents and sea level adjustment off the west coast of South Island, New Zealand. *Journal of geographical research.*

Tabata, S. 1976: The general circulation of the Pacific Ocean and a brief account of the oceanographic structure of the North Pacific. *Atmosphere 14*: 1–27.

U. S. Navy 1981: Marine climatological atlas of the world, Vol. 9. *NAVAIR document 50–1C–65, Washington.*

Woods, J. D.; Barkmann, W. 1986: The response of the upper ocean to solar heating. I: The mixed layer. *Quarterly journal of the Royal Meteorological Society 112*: 1–27.